# DETERMINATION OF THE MODAL DISPERSION CURVES IN A NOISY SHALLOW WATER WAVEGUIDE

**D. Cassereau[a], P. Roux[b], and F.-D. Philippe[a]**
[a] Laboratoire Ondes et Acoustique, Université Paris 7 - CNRS UMR 7587 - ESPCI, Paris, FRANCE
[b] Marine Physical Laboratory - Scripps Institution of Oceanography, La Jolla, U.S.A.
didier.cassereau@espci.fr

## Abstract

In this paper, we are interested in the determination of the modal dispersion curves that describe the propagation of sound in a shallow water waveguide like the ocean. We shortly describe the inversion method and show how we can reduce the influence of the noise on experimental or simulated data, using a holographic array processing technique from an array of receivers. Then we show how the inversion method can be used to obtain the modal dispersion curves.

## Introduction

Wave propagation in a shallow water oceanic environment is usually considered in the general frame of acoustic waveguides. The determination of the waveguide properties without any a priori knowledge of the environment is well-known to be a difficult task. More particularly, the measurement of the waveguide wavenumbers from a synthetic aperture array usually requires high-resolution algorithm. In the recent past, various algorithms have been proposed to determine the wave numbers from experimental or simulated data, like the Prony algorithm [1] or the matrix pencil method [2]. Recently, we proposed and evaluated an alternate wave number inversion method that proved its efficacy in terms of accuracy and computation time [3]. In this work, we use our algorithm to calculate from time-domain simulated data the dispersion curves that describe modal propagation in the waveguide. To this goal, we consider a towed source that transmits regularly a pulsed signal received after propagation through the waveguide on an array of receivers. From the received transient signals, we calculate the wavenumbers for all frequencies inside the bandwidth of the source-receiver system. This procedure provides the modal dispersion curves corresponding to the different modes in the waveguide in the considered bandwidth.

Another important parameter of the problem is the influence of the noise level on the determination of the wavenumbers. We numerically investigate the robustness of the inversion algorithm as a function of the signal-to-noise ratio. We finally combine our inversion technique with a noise reduction method based on holographic array processing [4].

## Basic principles

In underwater acoustics, the pressure field $P_\omega$ at a frequency $f = 2\pi\omega$ is decomposed under the propagating modes as follows:

$$P_\omega(R) = \sum_{m=1}^{M} a_m \exp(ik_m R), \qquad (1)$$

where $M$ is the number of modes, $R$ is the source-receiver range, and $k_m$ is the wavenumber associated to mode $m$. For simplicity, we neglect the attenuation in the waveguide.

Like in many high-resolution techniques, the data are issued from a towed source providing a horizontal synthetic aperture; for the $n^{\text{th}}$ position of the source given by $R=R_0+nd$, we measure the corresponding pressure $P_\omega[n]$ received on the receiver.

Replacing $R$ in (1) by its expression, we obtain an equivalent formulation of (1) as

$$P_\omega[n] = \sum_{m=1}^{M} \tilde{a}_m z_m^n \text{ , with } z_m = \exp(ik_m d). \qquad (2)$$

In this equation, we have $M$ unknown amplitudes $\tilde{a}_m$ and $M$ unknown phases $z_m$. Consequently, we need at least $2M$ data points in order to solve this system. Using $2M$ data points, the problem can be seen as the inversion of the following $2M$-equation system:

$$\begin{cases} P_\omega[0] & = \tilde{a}_1 + \tilde{a}_2 + \cdots + \tilde{a}_M \\ P_\omega[1] & = \tilde{a}_1 z_1 + \tilde{a}_2 z_2 + \cdots + \tilde{a}_M z_M \\ \cdots & \\ P_\omega[M-1] & = \tilde{a}_1 z_1^{M-1} + \tilde{a}_2 z_2^{M-1} + \cdots + \tilde{a}_M z_M^{M-1} \\ \cdots & \\ P_\omega[2M-1] & = \tilde{a}_1 z_1^{2M-1} + \tilde{a}_2 z_2^{2M-1} + \cdots + \tilde{a}_M z_M^{2M-1} \end{cases} \qquad (3)$$

The system described by (3) is linear with respect to $\tilde{a}_m$, but it is highly nonlinear with respect to $z_m$. This nonlinearity makes the inversion difficult and highly sensitive to noise.

Several high-resolution techniques can be used to invert for the phases $z_m$ (matrix-pencil methods, Prony algorithm). We propose an approach that is similar to the Prony method. Our algorithm is based on the following steps:

- we start from the first $M$ equations of (3), and write the $\tilde{a}_m$ as a function of the data $P_\omega[n]$ and phases $z_m$,

- we continue with the last $M$ equations of (3), in which the $\tilde{a}_m$ are replaced by their expression.

These two steps are symbolic manipulations of (3); there is no numerical treatment here. Of course, we obtain a system of $M$ equations with $M$ unknown phases $z_m$, that is highly nonlinear. Anyway, we can show that this system is linear with respect to the Elementary Symmetric Polynomials defined by:

$$E_1 = \sum_{i=1}^{M} z_i, E_2 = \sum_{i=1}^{M}\sum_{j=i+1}^{M} z_i z_j, \ \ldots, E_M = \prod_{i=1}^{M} z_i \ . \qquad (4)$$

After a change of variable from the $z_m$ to the $E_m$, the linear system to be inverted can be written as:

$$\begin{cases} P_\omega(M) = P_\omega(M-1)E_1 - P_\omega(M-2)E_2 + \cdots (-1)^{M-1} P_\omega(0)E_M \\ P_\omega(M+1) = P_\omega(M)E_1 - P_\omega(M-1)E_2 + \cdots (-1)^{M-1} P_\omega(1)E_M \\ \ldots \\ P_\omega(2M-1) = P_\omega(2M-2)E_1 - P_\omega(2M-3)E_2 + \cdots (-1)^{M-1} P_\omega(M-1)E_M \end{cases}$$

The next steps of our inversion algorithm are:
- numerical inversion of the last linear system and computation of the $E_m$,
- calculation of the phases $z_m$ as the complex roots of a degree-$M$ polynomial, whose coefficients are the $E_m$.

The determination of the $E_m$ results from the inversion of a linear system; thus there is no particular difficulty here in the numerical implementation. Then the final resolution step reduces to the search of the roots of a polynomial, which can be performed from multiple and stable numerical algorithms. In fact, the most complex step was the symbolic manipulations that were needed to obtain the last formulation given above.

**The holographic array processing**

As every nonlinear inversion technique, our approach is highly sensitive to the signal-to-noise ratio (SNR). Since ocean experimental data is usually quite noisy, we must take into account this parameter.

Instead of considering a single receiver, we now use an array of receivers that cover the whole water depth. To improve the SNR, we use holographic array processing that consists in cross-correlating the field coming from an unknown source to the field coming from a reference source. The first point of the source track is chosen here as the reference source. The cross-correlated fields are then summed over the vertical aperture. This process results in a coherent combination of the acoustic field on the array. This leads to an increase of SNR on the order of $10\log_{10}(K)$, where $K$ is the number of elements on the array. Holographic array processing replaces the data points $P_\omega[n]$ by a new variable $H_\omega[n]$ that can be decomposed in the same way as (2). As an immediate consequence, the inversion method described above remains unchanged.

**Representation of the multi-valued solutions**

As described in the two previous sections, our inversion method (with or without holographic array processing) yields the numerical determination of the phase variables $z_m = \exp(ik_m d)$. Now, the calculation of the corresponding $k_m$ is not straightforward, even in the case of a well-known distance $d$. This is due to the fact that the phase of a complex number is known, up to a multiple of $2\pi$. As an immediate consequence, the wavenumbers $k_m$ are given by

$$k_m d = phase(z_m) + 2p\pi \ , \qquad (5)$$

where $p$ can be any positive or negative integer.

In order to find the exact wavenumbers, we take advantage of the large number of data points. Indeed, our inversion algorithm is performed from $2M$ data points, and we can choose multiple subsets of $2M$ equally points in the total aperture $L$ covered by the moving source. We finally proceed in the following manner:
- we choose $d$ and a subset of $2M$ data points such that we have $(2M\text{-}1)d<L$, on which we run our inversion algorithm.
- once the $z_m$ are known, we calculate all possible values of $k_m$ inside a reasonable range, taking into account the multi-valued solutions,
- we restart the last two steps for all possible subsets of points for a given value of $d$, and also for different values of $d$ if possible.

The basic idea of this procedure is to cumulate the multi-valued wavenumbers obtained from different subsets of data points, and draw a histogram of all possible solutions. For an effective solution, all individual histograms will have a peak at the same $k$-position, thus resulting in a cumulative high peak on the final result. For a non-pertinent solution resulting from the multi-valuation, it will be spread along the $k$ axis from one particular histogram to another one, and we do not expect to see any peak in this case.

As a matter of fact, a strong peak detection on the final histogram allows to separate the actual solution from virtual solutions that result from multi-valuation.

**Numerical results**

Data are obtained from a numerical simulation in a 60-m deep Pekeris waveguide using the Kraken normal mode code at a frequency of 200 Hz. The bottom sound speed, density and attenuation are 2000 m/s, 2000 kg/m$^3$ and 0.1 dB/$\lambda$. The source is towed away from the receiver on a total aperture $L$=1500 m with an initial distance to the receiver $R_0$=3000 m; the depth of the source is 15 m. The water sound speed and density are 1500 m/s and 1000 kg/m$^3$.

Fig.1 shows a typical cumulative histogram obtained from our inversion technique with a single receiver in

the absence of noise. The sharp peaks correspond to the actual modes in the waveguide, in the range [0.55 $m^{-1}$-0.95 $m^{-1}$]. The portion of the histogram between 0.85 and 0.95 $m^{-1}$ gives us an estimation of the average noise level resulting from the multi-valuation treatment. We then define a threshold with respect to this average noise level in order to detect the peaks in the histogram.

In Fig. 1, we clearly identify 11 different peaks that rise high above the average noise level. These different peaks correspond to the actual wavenumbers of the waveguide.

In Fig. 2, random white noise is added on the simulated data points (SNR=20 dB). Comparing Figs. 1 and 2, we see that the detection of modes is more difficult in the presence of noise; the average noise level does not change between the different figures, but the height of the peaks decreases as noise increases. Some peaks are no more detected, and the two highest modes can not be distinguished, as in Fig. 1. If we use a detection based on a threshold compared to the average noise level, we can expect that some modes are missed in the case of a highly noisy propagation in the waveguide.

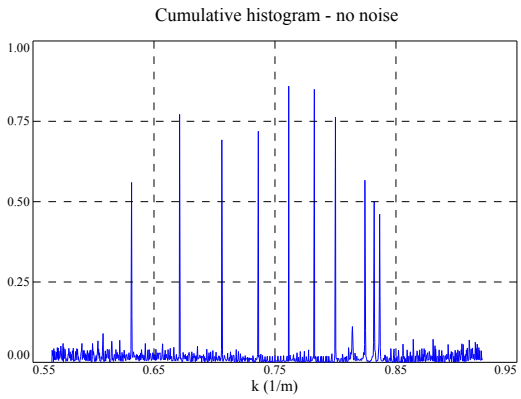


Figure 1: typical cumulative histogram without noise.

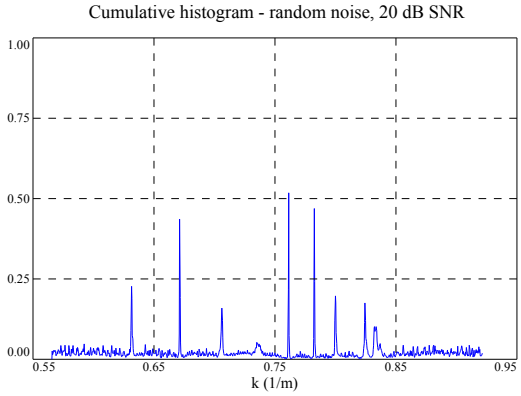


Figure 2: same as figure 1, with a random white noise, 20 dB SNR.

In order to increase the signal-to-noise ratio and allow a better detection, we apply the same inversion procedure using holographic array processing on the receiver array. A set of 19 receivers covers the water depth in the waveguide between 3 m and 57 m; the distance between two successive receivers is 3 m.

Fig. 3 represents the corresponding cumulative histogram for a 20-dB SNR. We observe a better peak detection than in the case of a single receiver. Also, the two highest peaks can now be distinguished. This illustrates how holographic array processing takes advantage of the large number of receivers to increase the signal-to-noise ratio, and thus to improve the determination of the wavenumbers in the waveguide.

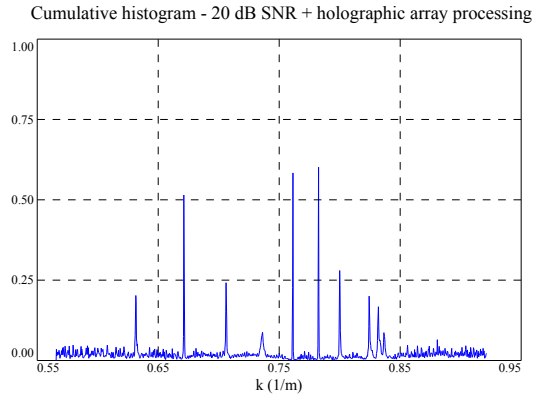


Figure 3: same as figure 2, using 19 receivers.

**Variation of the wavenumbers with receiver depth**

From the above procedure, we are able to determine the propagation modes of the waveguide for a particular depth of the source and receiver. It is interesting to see how the mode detection varies with the depth of the receiver, in order to check that the inversion does not depend on this parameter.

For that purpose, we run the inversion algorithm separately for each of the 19 receivers in the absence of noise. In Fig. 4, the detected wavenumbers are shown for a single receiver between 3 m and 57 m. The curves reduce to vertical straight lines, and this effectively confirms that our detected wavenumbers do not change from one receiver to another. However, we observe that some wavenumbers are lost for particular receivers. This occurs when the receiver is located near a node of a specific mode; consequently the corresponding mode can not be detected at this position.

**Modal dispersion curves in the ocean**

In the previous sections, we considered only mono-chromatic signals at the frequency of 200 Hz. The simulated data points have been calculated using a single-frequency propagation model.

We investigate now the case of broadband signals received from a horizontal synthetic aperture. To do so, the previous inversion procedure is repeated for all the frequencies that are effectively present in the

temporal signals received on the array. This yields a series of wavenumbers for each frequency that can be represented in the $(k, f)$ space to obtain the modal dispersion curves of the waveguide. These dispersion curves are very important because they contain much information about the physical properties of the waveguide and bottom.

In practice, the simulated data points are now obtained from a transient propagation model based on the Kraken normal mode code. The central frequency is 200 Hz, and the effective bandwidth is in the range [175-225 Hz]. The computation of the dispersion curves has been limited to this frequency range. The length of the horizontal aperture $L$=1500 m is the same as before.

The complete procedure is now the following:

- for a given frequency $f$, we calculate a discrete Fourier transform of the time-domain received signals for every point of the horizontal synthetic aperture,
- then we run the inversion procedure as described in the previous section; the cumulative histogram is replaced by a mode detection, using a threshold defined by the average noise level calculated from the up-front portion of the histogram.

Figs. 5a and 5b show the modal dispersion curves obtained in the absence of noise and in the case of a 20-dB SNR, respectively. On these two figures, we see the classical structure of the dispersion curves in the waveguide, and the degradation due to the presence of noise.

## Conclusion

In this work, we have presented a numerical procedure to calculate the propagating wavenumbers in a waveguide, and the resulting dispersion curves. These results may be useful in underwater acoustics, since dispersion curves contain information about the waveguide properties.

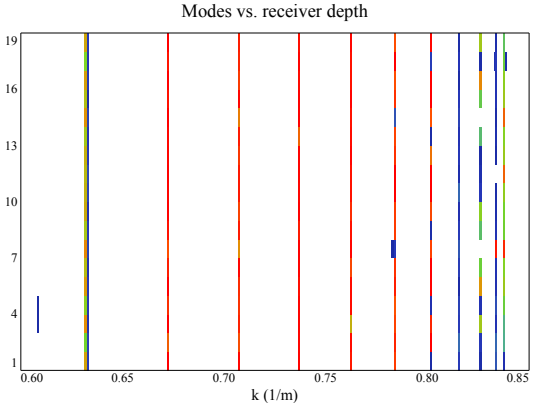


Figure 4: variation of the modes with receiver depth.

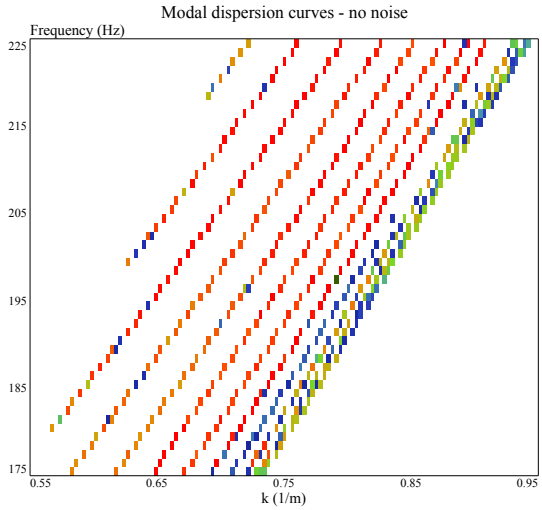


Figure 5a: dispersion curves without noise.

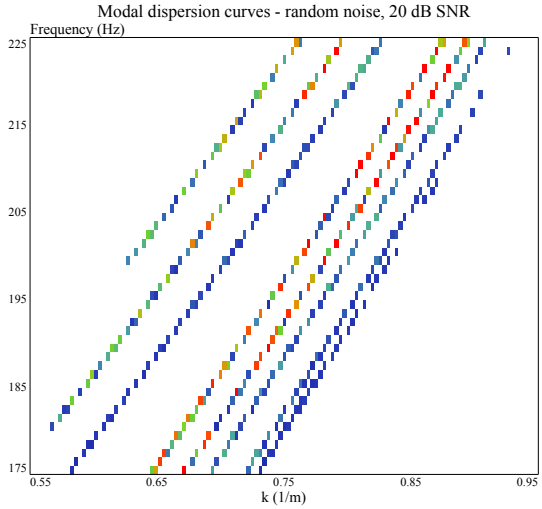


Figure 5b: dispersion curves with a 20-dB SNR.

## References

[1]. S.M. Kay and S.L. Marple, "Spectrum analysis – A modern perspective", Proc. IEEE 69, 1380 (1981),

[2]. Y. Hua and T.K. Sarkar, "Matrix pencil method for estimating parameters of exponentially damped/undamped sinusoids in noise", IEEE Trans. Acoust., Speech, Signal Process. 38 (5), pp. 892-900, 1990,

[3]. P. Roux, D. Cassereau and A. Roux, "A high-resolution algorithm for wavenumber estimation using holographic array processing", to be published in the J. Acoust. Soc. Am.,

[4]. Martin Siderius, Darrel R. Jackson, Daniel Rouseff and Robert P. Porter, "Multipath compensation in shallow water environments using a virtual receiver", J. Acoust. Soc. Am. 102(6), pp. 3439-3449, 1997.